IEEE Access
Multidisciplinary | Rapid Review | Open Access Journal

SPECIAL SECTION ON COLLABORATION FOR INTERNET OF THINGS

Received July 27, 2018, accepted August 22, 2018, date of publication August 31, 2018, date of current version October 8, 2018.

Digital Object Identifier 10.1109/ACCESS.2018.2868227

Application of Multi-Sensor Image Fusion of Internet of Things in Image Processing

HONG LI, SHUYING LIU, QUN DUAN, AND WEIBIN LI
School of Computer Science, Xianyang Normal University, Xianyang 712000, China

Corresponding author: Hong Li (honglishining@163.com)

This work was supported in part by the National Natural Science Foundation of China under Grant 81473559, in part by the Natural Science Basic Research Plan in Shaanxi Province of China under Grant 2017JM6086, in part by the Science Basic Research Program in Shaanxi Province of China under Grant 16JK1823, in part by the Innovation Program in Shaanxi Province of China under Grant 2018KRM145, in part by the Science Basic Research Program in Xianyang Normal University of China under Grant XSYK18012, in part by the Students' Platform for Innovation and Entrepreneurship Training Program in Shaanxi Province of China under Grant 201828003, and in part by the Students' Platform for Innovation and Entrepreneurship Training Program in Xianyang Normal University of China under Grant 2018014.

ABSTRACT The perception layer of Internet of Things (IOT) consists of various sensors. It is the source of the IOT to identify objects and collect information. Information fusion collected from multi-sensor has been widely used in various fields, such as intelligent industry, intelligent agriculture, intelligent transportation, and intelligent environmental protection. In this paper, multi-sensor image fusion, multispectral (MS) and panchromatic (PAN) images, is studied, and the fused images are used in target detection, recognition, and classification. However, traditional methods based on an injection model generally consider the MS images as a whole to compute the spectral weights. They ignore the local information of MS images and produce some spectral distortions, because for different objects, the spectral response will be different. Therefore, we propose a novel multi-sensor image fusion based on application layer of IOT (IFIOT) to preserve the spectral information of MS images. In this method, local homogeneous areas are found first by superpixel segmentation. Due to good properties of superpixel, the homogeneous areas are uniform and contain only one kind of object. Then, we estimate the spectral weights for different bands on the homogeneous area. The injection gain has an important influence on fusion results. Therefore, we adaptively compute the gain coefficients by minimizing the error between the spectral degraded MS and PAN images. Finally, after the injection of spatial details obtaining from the PAN image, fused images are produced. Experimental results reveal that the IFIOT method can give good fusion results and the spectral information is preserved well.

INDEX TERMS Internet of Things, multisensor, image fusion, homogeneous region, adaptive gain.

I. INTRODUCTION

With the development of wireless sensor network with computing ability and communication ability, smart visual Internet of Things (IOT) has been widely used in various fields [1], [2]. The IOT architecture includes perception, network and application layers. Perception layer consists of different sensors, including temperature and humidity sensor, RFID tag and reader, camera, infrared ray, GPS etc. A large number of sensors of various types are deployed on the IOT. Information content obtained by different sensors can satisfy the requirement of collection and compression of multimedia information like images, audios and videos in practical applications. Network layer is the core of IOT, and it has different networks, such as internet, network and cloud computing platform etc. The main task of the network layer is the processing and transmission information. Application layer is an interface of users and IOT, which meets the users' needs to realize the smart application of IOT. Remote sensing is a non-contact remote detection technology that monitor the earth's surface by installing remote sensing monitoring instruments on satellites. At present, with the rise and development of IOT, the application of remote sensing monitoring and IOT technology has also presented a new development trend, such as target detection, recognition and classification [3]–[5] etc. In recent years, many satellites are launched into space. At the same time, a large amount of remote sensing data are obtained by these satellites, such as multispectral (MS) images and panchromatic (PAN) image. However, the limitation of spectral resolution and spatial resolution always exists because of remote sensing technology.

2169-3536 © 2018 IEEE. Translations and content mining are permitted for academic research only.
Personal use is also permitted, but republication/redistribution requires IEEE permission.
See http://www.ieee.org/publications_standards/publications/rights/index.html for more information.

For example, MS images usually contain abundant spectral information, but its spatial resolution is poor. On the contrary, PAN image can provide clear spatial characteristics with high spatial resolution. However, it only contains one channel and there is no spectral information for the observed objects. Therefore, remote sensing image fusion is proposed to integrate the complementarity and advantages of different images to obtain high spectral and spatial resolution MS (HMS) images. This process is also named as pansharpening.

Because of the satisfactory performance, image fusion has been developed a lot over the last few decades. Thus, many classical approaches have been proposed [6]–[31]. For example, two methods, principal component analysis (PCA) [6] and intensity-hue-saturation (IHS) [7] transformation, are proposed to enrich the spatial details of MS images. In 2000, Gram-Schmidt (GS) [8] transformation is also proposed, which is similar to PCA and IHS strategies. After all these, some improved versions of these methods are proposed to produce better fusion results. For example, the fast IHS and adaptive GS are also proposed in [9] and [10]. These methods are used widely because of its easily implement and speedily computation. However, the spectral information of the fusion results of these methods usually cannot be preserved well and obvious spectral distortions can be seen from the fused images [11]. Subsequently, some methods [12]–[17] are proposed to enhance the performance of image. Compared with the above approaches, the methods based on spatial detail injection attract broader attention in remote sensing community. These methods assume that the spatial details of MS images can be found in PAN image and the spatial details of PAN image are extracted and then injected into MS images to obtain clear HMS images. In [14], authors use wavelet as a tool to extract the spatial details. In [15], contourlet is used to find proper high frequencies of PAN image, which first find the most similar component by adaptive-PCA. In [16], á trous algorithm, which is an undecimated wavelet transform, is used to avoid the spatial aliasing. The algorithm also produces good fusion results. Because of the advantages in spectral features, these methods are widely studied. However, the spatial distortions are obvious in the fused images of some methods and some spatial aliasing effect can be seen.

Recently, some novel approaches are proposed to find more proper spatial details to avoid the spatial aliasing [18]–[27]. For example, a novel method based on compressed sensing is proposed, which imposed the sparse constraint on the coding coefficients and produced good fusion results [19]. Then, some improved version based on these methods are proposed [20]–[25]. Li *et al.* [21] use dictionary learning technique to learn original dictionaries from original PAN and MS images. Meng *et al.* [23] give a fusion algorithm based on guided filter. Firstly, PAN is decomposed into detail, edge, and low-frequency layers. Information of the first two layers are then injected into MS images. Li *et al.* [24] propose a refined fusion measure using NSCT and hierarchical sparse auto-encoder. For PAN image, directional details are extracted in each scales via NSCT. Then, these details are gradually purified by hierarchical sparse auto-encoder. In [25], non-negative matrix factorization (NMF) is applied to pansharpening strategy. PAN and MS are represented by sparse NMF to construct the coupled SNMF model.

Besides, in recent years, fusion measures based on kernel method [28] and adaptive methods [29]–[31] are proposed to improve the performance of sharpened images. Li *et al.* [28] propose fusion method via local geometrical similarity, which the steerable kernel is used to calculate the similarity coefficients in a local window. Delleji *et al.* [29] propose an adaptive fusion measure. In each segmentation map, the correlation is computed. Choi *et al.* [30] use a local and a global context-adaptive parameter, which is computed by spatial correlation of intensity and MS images. Finally, fusion quality is optimized adaptively via image entropy. Experimental results demonstrate these methods are effective in the field of remote sensing image fusion.

Injection model are efficient and can improve the spatial information of MS images. However, due to the methods based on component substitution model always consider MS images as a whole to find the corresponding spectral coefficients, which ignore the local information for different kinds of objects and lead to spectral distortions. For example, the spectral weights of tree area will be not consistent with those of building area or road area. In other words, for different homogeneous area, the spectral weights will be different. Here, the homogeneous area generally stands for the area containing one kind of object. Therefore, we propose a novel multi-sensor image fusion based on application layer of IOT (IFIOT). IFIOT adaptively compute the corresponding weights for each band in different homogeneous areas. Then, superpixel technique [32] is used to find a proper homogeneous area. Superpixel aims at segmenting different objects in images and find uniform regions, which has been used widely on many computer vision tasks such as object detection and image classification. After segmented the whole image into different homogeneous areas, the gains for different bands are computed. Then, the proper details from PAN image are injected into MS images to produce HMS images.

Compared with available image technologies, the contribution of our work is: 1) IFIOT is advanced to segment the different object and find a proper homogeneous area; 2) For different areas, the adaptive gain idea also helps to improve the results of our method by using the relationship between PAN and spectral degraded MS images. Consequently, the spectral and spatial distortion can be minimized in obtained HMS images. Some experiments are taken on several datasets, and experimental results reveal that the proposed IFIOT measure outperforms its counterparts.

The remainder of this paper is organized as follows. Section II, injection model is described in details and IFIOT approach is proposed. Section III, some experiments are implemented on two datasets. Then some conclusions are concluded in Section IV.

II. MULTI-SENSOR IMAGE FUSION BASED ON APPLICATION LAYER OF IOT

We first describe the framework of injection model [33] for image fusion task, and then describe the proposed method based on application layer of IOT, which the core idea is superpixel and adaptive gain in detail.

A. INJECTION MODEL

We use to $\mathbf{M} \in R^{rN_r \times rN_c}$ stand for MS images. $\mathbf{M}_b$ $(b = 1, \ldots, B)$ is each band of MS images. B is the number of bands of MS images. $\mathbf{P} \in R^{N_r \times N_c}$ denotes PAN image. N_r and N_c are the horizontal and vertical size of PAN image. r is the spatial resolution ratio between MS and PAN images. For MS and PAN images fusion, we consider the case that MS images contain four bands, since the number of bands is 4 for most satellites. According to the injection model theory, the formulation can be written as:

$$\hat{\mathbf{M}}_b = \tilde{\mathbf{M}}_b + g_b \mathbf{D}_b \tag{1}$$

In (1), $\tilde{\mathbf{M}}_b$ is the resampled band of MS images, and the size of $\tilde{\mathbf{M}}_b$ is the same size of PAN image. $\widehat{\mathbf{M}}_b$ denotes the fused band. g_b is the corresponding gain coefficient for each band, which is decided by the spectral and spatial information jointly. $\mathbf{D}_b$ is the spatial details to be injected, which is also named as high frequency information. Then, the injection model can be written as:

$$\hat{\mathbf{M}}_b = \tilde{\mathbf{M}}_b + g_b \left(\mathbf{P} - \sum_{b=1}^{B} w_b \tilde{\mathbf{M}}_b \right) \tag{2}$$

where w_b is the corresponding spectral weight of each band. By combining the bands in MS images with different weights, a simulated intensity image is obtained. Then, the spatial details $\mathbf{D}_b$ can be produced by the difference of PAN and simulated intensity images. For different band, the injection gain g_b will be different. Generally, MS and PAN images are all considered to decide the gain coefficients. For instance, spectral weights are computed by least square in the minimum mean-square-error sense in [34]. However, the weights are computed for the whole image and ignore the local consistency. Because for different local areas contains different objects, the spectral weights will be different. Therefore, some spectral distortions maybe can be seen from the fusion results.

B. MULTI-SENSOR IMAGE FUSION BASED ON APPLICATION LAYER OF IOT

It is obvious that using a fixed spectral weight is not feasible for a whole image. For different homogeneous areas, the spectral weights will have great differences. Therefore, we first have to find the homogeneous area which contains one kind of object. There are some methods to be used to find proper areas. For example, some methods find the areas by clustering with intensity and local standard deviation [35]. However, the method maybe produce some spectral distortions due to the uncertainty of standard deviation. On the contrary, as a segmentation technique, superpixel has been developed a lot and can find uniform area effectively. Therefore, in our method, superpixel is used to find the homogeneous areas. In [32], a superpixel method based on entropy rate is proposed which presented a new graph construction method for images and produce more natural segmentation results. So, we adopt the method to segment PAN image into many homogeneous areas. This objective function of the superpixel method is composed of two parts. One is entropy rate of a random walk on a graph. The other is a balancing term. They can be efficiently implemented and give the state of the art segmentation results.

The areas in PAN image can be denoted as $\mathbf{P}^k (k = 1, 2, \ldots, K)$ after superpixel segmentation. K is the total number of superpixels in PAN image and k is the k-th superpixel in PAN image. Then, the corresponding areas of MS images can be find using PAN image according to the pixel locations in PAN image. We use $\tilde{\mathbf{M}}_b^k$ to denote the superpixel in each band of $\tilde{\mathbf{M}}_b$. After finding the homogeneous areas, we calculate the spectral weights from the resampled MS images $\tilde{\mathbf{M}}$ and the spatial degraded PAN image $\tilde{\mathbf{P}}$. And $\tilde{\mathbf{P}}$ is produced by the operation with the low-pass filter. The corresponding superpixel of $\tilde{\mathbf{P}}$ is $\tilde{\mathbf{P}}^k$. Then, for the$k$-th superpixel, the spectral weights of MS images can be calculated by minimizing (3).

$$\min \left\| \tilde{\mathbf{P}}^k - \sum_{b=1}^{B} w_b^k \tilde{\mathbf{M}}_b^k \right\|_2^2 \tag{3}$$

where $\tilde{\mathbf{P}}^k$ and $\tilde{\mathbf{M}}_b^k$ are rearranged a vector. Obviously, the spectral weights w_b can be easily calculated by least square method. w_b^k stands for the spectral weight on each band for the k-th superpixel. Then, we inject the spatial details into the resampled MS images by (4).

$$\hat{\mathbf{M}}_b^k = \tilde{\mathbf{M}}_b^k + g_b^k \left(\mathbf{P}^k - \sum_{b=1}^{B} w_b^k \tilde{\mathbf{M}}_b^k \right) \tag{4}$$

Obviously, gain coefficient g_b^k is important in the image fusion process. Proper gain coefficients can preserve the spectral information well. As we all know, PAN image can be considered as the degraded result of HMS images in spectral domain. So, when obtain an HMS images, we hope the difference between PAN and the spectral HMS is minimum. Then, the assumption can be written as:

$$\min \left\| \mathbf{P}^k - \sum_{b=1}^{B} w_b^k \left(\tilde{\mathbf{M}}_b^k + g_b^k \left(\mathbf{P}^k - \sum_{b=1}^{B} w_b^k \tilde{\mathbf{M}}_b^k \right) \right) \right\|_2^2 \tag{5}$$

According to (3), we can know $\tilde{\mathbf{P}}^k \approx \sum_{b=1}^{B} w_b^k \tilde{\mathbf{M}}_b^k$. Therefore, after some simplification operations, the equation (5) can be written as:

$$\min \left\| \mathbf{P}^k - \tilde{\mathbf{P}}^k - \sum_{b=1}^{B} w_b^k g_b^k \left(\mathbf{P}^k - \tilde{\mathbf{P}}^k \right) \right\|_2^2 \tag{6}$$

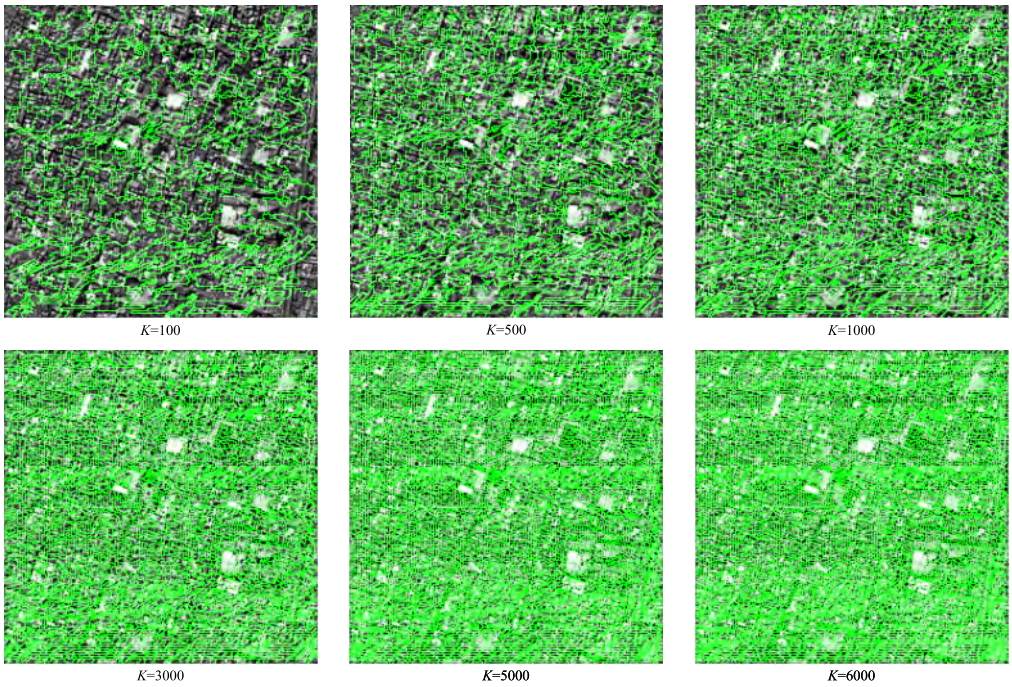

FIGURE 1. Different segmentation results for different K.

Then, make $\mathbf{P}^k - \tilde{\mathbf{P}}^k$ equal $\mathbf{e}^k$. We can compute by:

$$\min \left\| \mathbf{E}^k - \mathbf{E}^k \mathbf{W}^k \mathbf{g}^k \right\|_2^2 \tag{7}$$

where $\mathbf{W}^k$ is the diagonal matrix composed of w_b^k for each band, respectively. $\mathbf{g}^k$ is a vector which contains g_b^k for different bands. $\mathbf{E}^k$ is a matrix containing B columns, and each column is $\mathbf{e}^k$. Obviously, the gain coefficient matrix $\mathbf{G}^k$ can be computed and the result is $\left(\mathbf{E}^k \mathbf{W}^k\right)^\dagger \mathbf{E}^k = \mathbf{g}^k$. $\dagger$ stands for the pseudo inverse operation of a matrix. Therefore, after estimating the gain coefficients adaptively, the fused images can be produced by (4). The main steps of IFIOT method are listed as follows.

Algorithm 1 Multi-Sensor Image Fusion Based on Application Layer of IOT (IFIOT)

Input: PAN image $\mathbf{P}$ and MS images $\mathbf{M}$
Step 1: Produce the resampled MS image $\tilde{\mathbf{M}}$
Step 2: Segment PAN image into superpixels $\mathbf{P}^k$ $(k = 1, 2, \ldots, K)$
Step 3: Obtain corresponding superpixels of resampled MS image $\tilde{\mathbf{M}}_b^k$ $(k = 1, 2, \ldots, K)$
Step 4: for $k = 1{:}K$
  Calculate spectral weight w_b^k by (3)
  Compute gain coefficient g_b^k by (7)
  Produce the fused superpixels $\hat{\mathbf{M}}_b^k$ by (4)
  end
Step 5: Put the fused superpixels into orginal locations
Output: HMS images $\hat{\mathbf{M}}_b$

III. EXPERIMENTAL RESULTS

We use two data sets, collected from QuickBird and Geoeye-1 satellites, to evaluate IFIOT method. The size of MS and PAN is 256 × 256 × 4 and 1024 × 1024, respectively. In our work, simulation experiments are implemented. That is, all of the original images are decimated by 4. Then, pan-sharpening measures are performed on simulated data sets. IFIOT approach is compared with the six related measures, including GIHS [9], PCA [6], GS [8], DWT [36], AWLP [14] and TSSN [22]. In visual comparison, all the results are assessed by UIQI [37], SAM [38], Q_4 [39], RMSE [40] and ERGAS [40]. For UIQI, the value closer to 1 will be better. For Q_4, the value is between 0 and 1 and the best value is 1. For RMSE, SAM and ERGAS, best value is 0.

The number of superpixels K is very important. It affects the sharpened results. In our experiments, K is set as 5000. And the parameters of compared algorithms are seen on the related references.

A. ANALYSIS OF PARAMETERS

There is a parameter for on IFIOT: the number of superpixels K. Here, varies from 3000 to 6000 with the step of 500. We show the superpixel segmentation results of an image from QuickBird datasets in different number of superpixels in Figure 1. In order to more intuitively show the segmentation results, K is set as 100, 500, 1000, 3000, 5000, 6000, respectively. Then, the evaluation index values of fusion results from QuickBird dataset for different K are also shown in Table 1. In Table 1, R, G, B, NIR stands for red, green,

TABLE 1. Results of evaluation indexes for different K.

Metric	Band	3000	3500	4000	4500	5000	5500	6000
UIQI	R	0.8978	0.8979	0.8980	**0.8981**	**0.8981**	**0.8981**	**0.8981**
	G	0.8919	0.8920	0.8921	0.8922	0.8922	0.8922	**0.8923**
	B	0.8606	0.8606	0.8608	0.8608	**0.8609**	0.8608	**0.8609**
	NIR	0.9154	0.9156	0.9156	0.9157	**0.9158**	**0.9158**	**0.9158**
	Mean	0.8914	0.8915	0.8916	0.8917	**0.8918**	0.8917	**0.8918**
Q_4		0.8287	0.8288	0.8289	0.8289	**0.8290**	**0.8290**	**0.8290**
RMSE		24.3575	24.3648	24.3335	24.3306	**24.3216**	24.3221	24.3387
SAM		13.8794	13.8697	13.8662	13.8730	**13.8700**	13.8745	13.8748
ERGAS		4.1269	4.1251	4.1229	4.1225	**4.1210**	4.1211	4.1215

blue and near infrared bands of MS images. For a fixed image, if K is greater, the number of pixels in a superpixel will be less and for small superpixels, they generally contain one kind of object. But the computation complexity will be large and the calculation results of spectral weights will be not reliable. Therefore, bad fusion results will be produced. On the other hand, with the increase of K, the results about spectral weights and injection gains will be underdetermined and the bad fusion results will be produced due to the instability of weights and gains. On the contrary, if K is smaller, the number of pixels in a superpixel will be more. Then for a big superpixel, more kinds of objects will be contained in this superpixel. Naturally, for a non-homogeneous area, the spectral weights will be unreliable which leads to bad fusion results. From Figure 1, we can see that the size of superpixels will be smaller with the increasing of K, which means the possibility containing one kind of object will be larger. In Table 1, the best values of evaluation indexes are emphasize in bold font. From Table 1, we can see that the best values are produced when K is 5000. Although when K equals to 5500 and 6000, the UIQI values of evaluation indexes are the same as those of 5000, the values of other evaluation indexes are better than the results of 5500 and 6000. The values of evaluation indexes are consistent with the above analysis. So, K is set as 5000 in the following experiments.

B. INVESTIGATION ON THE PERFORMANCE OF IFIOT

We first discuss the investigation on the performance of IFIOT on several images. Figure 2 shows the injected details of different approaches. The first two columns are QuickBird datasets, and the next two columns are Geoeye-1 datasets. From top to bottom are the MS images, the injected details of GIHS, PCA, GS, DWT, AWLP and IFIOT, respectively. In Figure 2, the injected details of GIHS can barely be seen. Details of PCA is blurring and less informative. Details information extracted by GS, DWT and AWLP are more accurate than that of GIHS and PCA. Compared with all results, we can see IFIOT contains more accurate geometric structural because of using the local information to calculate spectral weights and adaptive gain.

C. FUSION RESULTS ON QUICKBIRD DATASETS

We fused the sources images from QuickBird datasets in this subsection. Sharpened results of different methods are shown in Figures 3-4. In Figures 3-4, MS, PAN and HMS images are shown in Figures (a)-(c), respectively. Figures (d)-(j) are arranged sharpened results of different approaches. Evaluation indexes are given in Tables 2-3. From Figure 3, we can see that there are some differences between the fusion results from different methods. For Figure 3 (d), the image is a little blurring and some spectral distortions exists. For Figure 3 (e), the result of PCA also suffers from some spectral distortions and the image is darker than the image of Figure 3 (d). Figure 3 (f) preserves color information well, but the spatial information in some areas is bad. Then, for Figure 3 (g), we can see the spatial information is clear but some spatial information look unnatural and some details are distorted. The fusion result in Figure 3 (h) is the same as the result in figure 3 (d). The result of TSSN produces a good image (see Figure 3 (i)). Compared with all results, we can see the result of IFIOT is the best. The spectral information is preserved well and the spatial information is clear. Then, we see the values of evaluation indexes in Table 2. The best value of SAM is given by GIHS. And IFIOT method gives the best values in UIQI, Q_4, RMSE and ERGAS, which means that the local homogeneous idea is valid. Because we consider the local information in source images by using superpixel technique, the result of IFIOT gives the best evaluation index values. Besides, the adaptive gain idea also help to improve the result of IFIOT method by using the relationship between PAN and the spectral degraded HMS images.

In Figure 4, similar results can be observed. For GIHS (Figure 4 (d)), we can see the spatial information is blurring. For PCA (Figure 4 (e)), the spatial information is clear and the result is darker. For GS (Figure 4 (f)), the spectral information is preserved well. For DWT (Figure 4 (g)), spatial information preserve well, but some spatial information look unnatural. Then, spatial information is a little burring in AWLP (Figure 4 (h)). The result of TSSN method (Figure 4 (i)) gives better spatial and spectral information. But the color region is darker. Compared with all results,

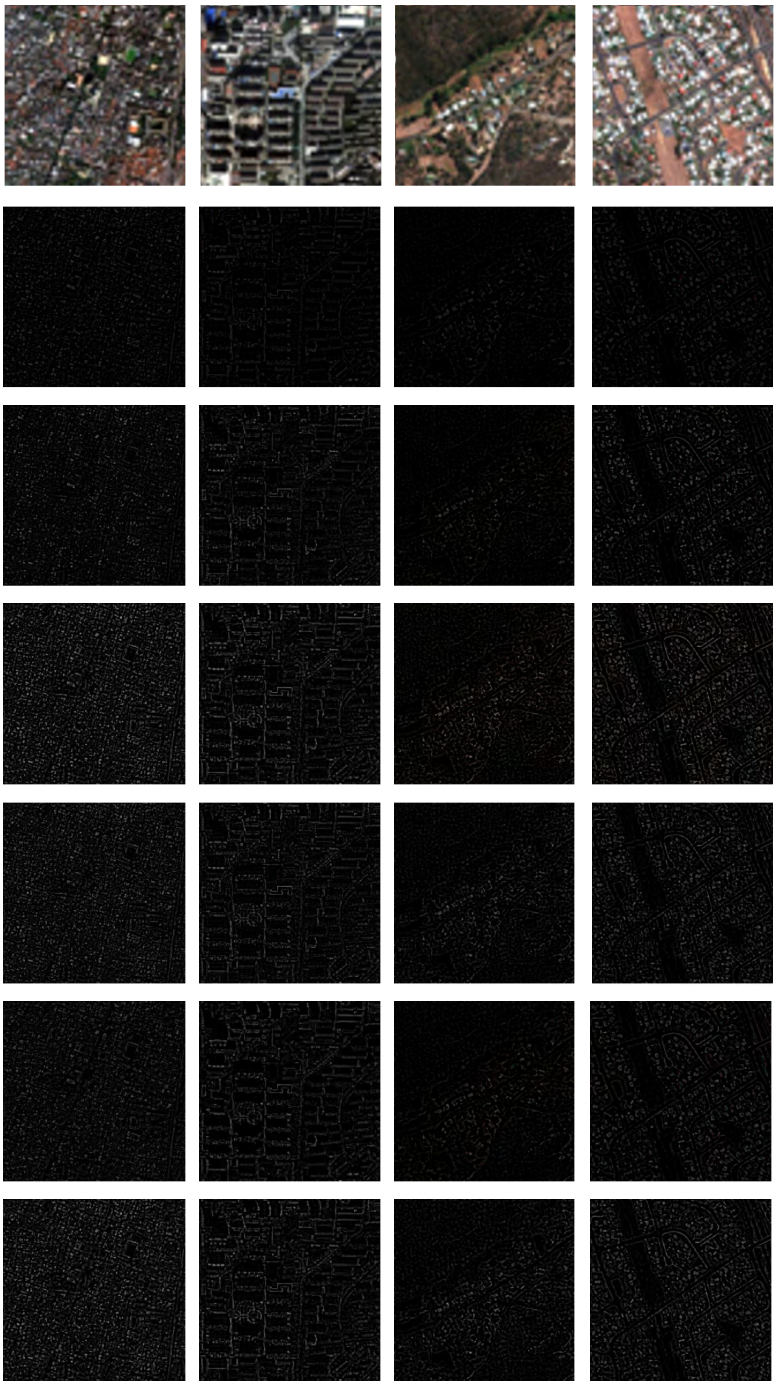

FIGURE 2. Injected details by different methods.

the result of IFIOT approach is closed to the reference HMS images. Evaluation indexes are listed in Table 3. We can see that GIHS and TSSN win in SAM and Q_4, respectively. However, IFIOT method gives the best UIQI, RMSE and ERGAS. From the fused images and the evaluation indexes, we can see that the local homogeneous idea is valid and the adaptive gain idea also help to improve the result.

D. FUSION RESULTS ON GEOEYE-1 DATASETS

Experiments are also performed on the Geoeye-1 datasets, which are shown in Figures 5-6. In Figures 5 and 6, MS, PAN and HMS images are shown in Figures (a)-(c), respectively. Figures (d)-(j) display the fused results of different strategies. Then, the values of evaluation indexes are given in Tables 4-5. We can see the spectral distortions are obvious and the color for different object is unnatural in Figure 5 (d).

TABLE 2. Results of evaluation indexes for different method in Figure 3.

Metric	Band	GIHS	PCA	GS	DWT	AWLP	TSSN	IFIOT
	R	0.7770	0.7333	0.8671	0.8149	0.8594	0.8593	**0.8981**
	G	0.7674	0.7199	0.8666	0.8082	0.8483	0.8557	**0.8922**
UIQI	B	0.7605	0.7055	0.8357	0.7817	0.8331	0.8146	**0.8609**
	NIR	0.8411	0.8118	0.9091	0.8886	0.8817	0.8991	**0.9158**
	Mean	0.7865	0.7426	0.8696	0.8233	0.8556	0.8572	**0.8918**
Q_4		0.6880	0.6612	0.8124	0.7670	0.7801	0.8183	**0.8290**
RMSE		29.1914	30.8387	27.8075	29.5231	26.9520	26.9086	**24.3216**
SAM		**12.1603**	12.2845	13.3419	14.7788	12.5702	14.8536	13.8700
ERGAS		4.9185	5.1964	4.6981	5.0054	4.5441	4.5575	**4.1210**

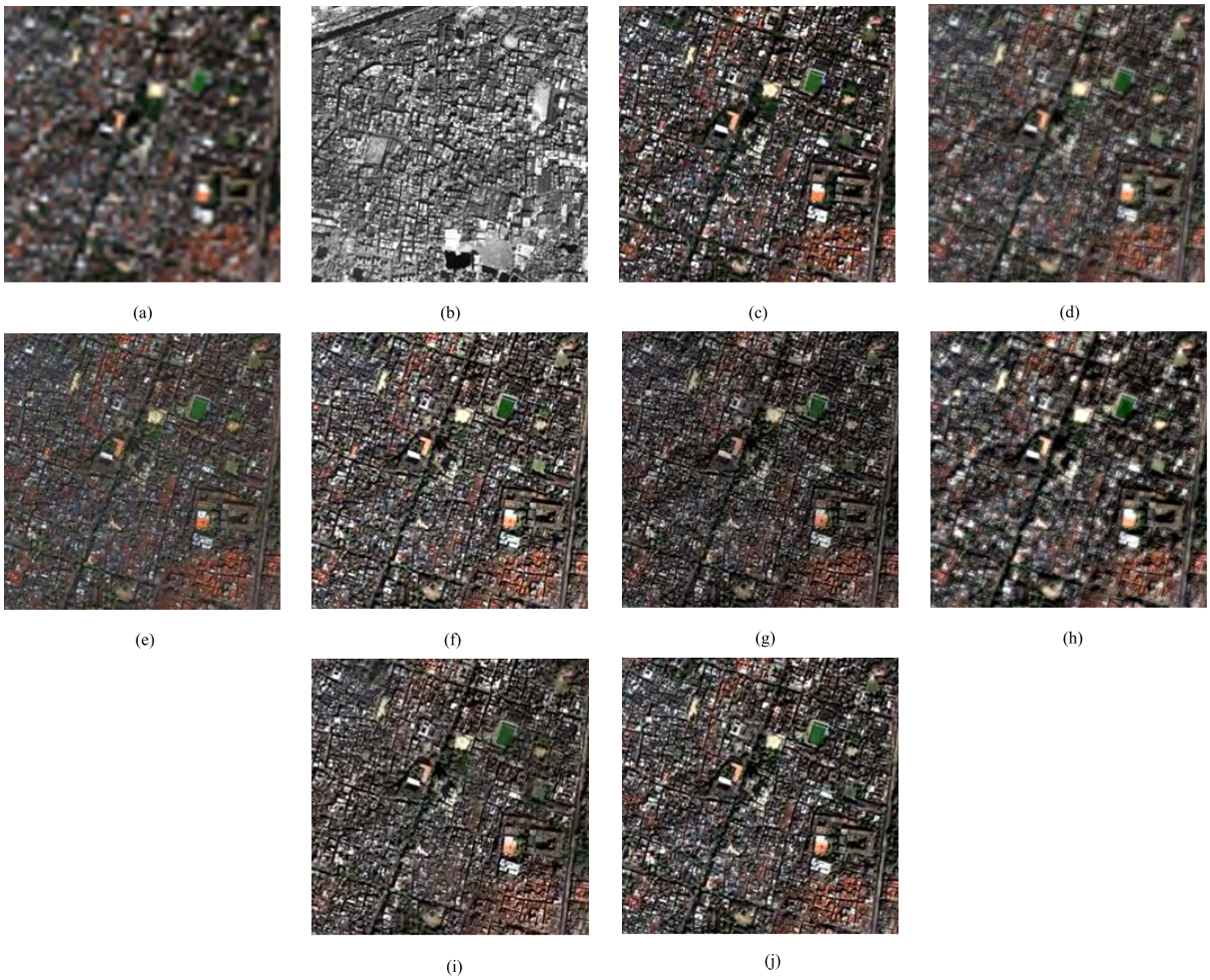

FIGURE 3. QuickBird Data Set. (a) MS, (b) PAN, (c) HMS, (d) GIHS, (e) PCA, (f) GS, (g) DWT, (h) AWLP, (i) TSSN, (j) IFIOT.

Figure 5 (e) shows that the intensity of the image is dark and some spatial information is blur. For Figure 5 (f), the result gives some distortions but it is better than the former two fusion results. We can see some spatial information is lost in Figure 5 (g) and some color distortions also can be found. Figure 5 (h) produces better color information, however, it looks unsharpness. Figure 5 (i) gives some better color information and the spatial details are also clear. But compared with the result of our proposed method, we can see the result of IFIOT method gives more natural color features for different objects and the spatial details are clear and proper. It is obvious that by using the local information to calculate

TABLE 3. Results of evaluation indexes for different method in Figure 4.

Metric	Band	GIHS	PCA	GS	DWT	AWLP	TSSN	IFIOT
UIQI	R	0.9260	0.9229	0.9432	0.9165	0.9128	0.9430	**0.9551**
	G	0.9244	0.9201	0.9416	0.9144	0.9109	0.9429	**0.9533**
	B	0.9215	0.9127	0.9328	0.8880	0.9015	0.9326	**0.9432**
	NIR	0.9380	0.9287	0.9386	0.8999	0.9002	0.9436	**0.9583**
	Mean	0.9275	0.9211	0.9390	0.9047	0.9064	0.9405	**0.9525**
Q_4		0.8455	0.8444	0.8708	0.8323	0.8428	**0.8856**	0.8835
RMSE		22.2136	21.7103	22.8907	25.7240	29.4661	20.3027	**18.4584**
SAM		**7.5265**	7.7136	7.7725	8.9001	8.0947	9.6888	8.2487
ERGAS		3.3578	3.2733	3.4335	3.8576	4.4158	3.0621	**2.7993**

FIGURE 4. QuickBird Data Set. (a) MS, (b) PAN, (c) HMS, (d) GIHS, (e) PCA, (f) GS, (g) DWT, (h) AWLP, (i) TSSN, (j) IFIOT.

spectral weights and adaptive gain, IFIOT can give better fusion results. From Table 4, we can see the best SAM is given by PCA. TSSN wins in Q_4. And other best values are produced by IFIOT, which further show that the effectiveness of the local information calculated superpixel technique.

Figure 6 shows fused results of the other Geoeye-1 datasets. The result of the GIHS is worse in spatial information, and the spectral distortions are obvious (see Figure 6 (d)). Figure 6 (e) shows that some spatial information is blur and the result is darker than reference HMS. For Figure 6 (f), the result gives some distortions but it is better than the former two fusion results. For Figure 6 (g), the spectral distortions are obvious, and the spatial information are serious lost. Figure 6 (h) gives some unnatural fused image.

FIGURE 5. Geoeye-1 Data Set. (a) MS, (b) PAN, (c) HMS, (d) GIHS, (e) PCA, (f) GS, (g) DWT, (h) AWLP, (i) TSSN, (j) IFIOT.

TABLE 4. Results of evaluation indexes for different method in Figure 5.

Metric	Band	GIHS	PCA	GS	DWT	AWLP	TSSN	IFIOT
UIQI	R	0.9146	0.9347	0.9049	0.9268	0.9296	0.9351	**0.9604**
	G	0.9192	0.9363	0.9027	0.9304	0.9260	0.9420	**0.9560**
	B	0.9045	0.9225	0.8820	0.8928	0.9155	0.9098	**0.9249**
	NIR	0.8594	0.8619	0.8706	0.7599	0.8361	0.8459	**0.9063**
	Mean	0.8994	0.9138	0.8901	0.8775	0.9018	0.9082	**0.9369**
Q_4		0.6921	0.7254	0.7598	0.7228	0.7655	**0.8052**	0.7854
RMSE		20.7560	16.6374	29.6221	24.4686	21.1820	18.0124	**15.3687**
SAM		6.3170	**5.7601**	6.8018	9.0145	6.7010	8.2434	7.3274
ERGAS		3.0663	2.3887	4.2967	3.2693	2.9706	2.6069	**2.2884**

And Figure 6 (i) produces poorly color information although the spatial details preserve well. Figure 6 (j), by contrast, is closed to reference HMS images. The result of IFIOT gives more natural color features for different objects and the spatial details are clear. Table 5 shows the evaluation indexes of the different approaches. It tells us that TSSN and PCA

FIGURE 6. Geoeye-1 Data Set. (a) MS, (b) PAN, (c) HMS, (d) GIHS, (e) PCA, (f) GS, (g) DWT, (h) AWLP, (i) TSSN, (j) IFIOT.

TABLE 5. Results of evaluation indexes for different method in Figure 6.

Metric	Band	GIHS	PCA	GS	DWT	AWLP	TSSN	IFIOT
UIQI	R	0.8709	0.9044	0.9238	0.9081	0.9170	0.9396	**0.9628**
	G	0.8613	0.8912	0.9119	0.8917	0.9071	0.9274	**0.9554**
	B	0.8548	0.8787	0.8838	0.8468	0.8950	0.8918	**0.9311**
	NIR	0.8733	0.8441	0.8696	0.7496	0.8372	0.8169	**0.8768**
	Mean	0.8651	0.8796	0.8973	0.8490	0.8890	0.8939	**0.9315**
Q_4		0.7162	0.7431	0.7804	0.7445	0.7877	**0.8202**	0.8155
RMSE		27.0270	25.1300	28.2651	34.3158	28.0752	24.5306	**20.2462**
SAM		6.4529	**6.4399**	6.9653	8.2272	7.2407	8.8167	6.6106
ERGAS		2.6221	2.4173	2.7179	3.3092	2.6904	2.3729	**1.9615**

give the best Q_4 and SAM, respectively. However, IFIOT method shows the best performance in UIQI, RMSE and ERGAS.

IV. CONCLUSIONS

Each sensor of the IOT is an information source, and the information content captured by different sensors

are different. In this paper, we propose a novel IFIOT approach to fuse the MS and PAN images. IFIOT strategy is focus on superpixel technique and adaptive gain. In our work, local homogeneous areas are considered and found by superpixel segmentation, to preserve the spectral information of MS images well. Then, spectral weights are calculated by the least square method. Subsequently, the injection gain coefficients are adaptively computed according to the relationship between MS and PAN images. Because of the considering of the local property, the fusion result of IFIOT method can preserve the color information well and the spatial information are also clear. From the results of evaluation indexes, such as UIQI, SAM, Q_4, RMSE and ERGAS, we also can see that IFIOT method produces a good fusion result. Thus, we can see the local homogeneous idea is valid and the adaptive idea also helps to improve the result of proposed method. In this paper, IFIOT method has been performed on multispectral data as the preferred application. For the future works, the framework can be applied to hyperspectral image sharpening.

REFERENCES

[1] L. Atzori, A. Iera, and G. Morabito, "The Internet of Things: A survey," *Comput. Netw.*, vol. 54, no. 15, pp. 2787–2805, Oct. 2010.

[2] J. Gubbi, R. Buyya, S. Marusic, and M. Palaniswami, "Internet of Things (IoT): A vision, architectural elements, and future directions," *Future Gener. Comput. Syst.*, vol. 29, no. 7, pp. 1645–1660, Sep. 2012.

[3] Y. Li, X. Sun, H. Wang, H. Sun, and X. Li, "Automatic target detection in high-resolution remote sensing images using a contour-based spatial model," *IEEE Trans. Geosci. Remote Sens.*, vol. 9, no. 5, pp. 886–890, Sep. 2012.

[4] L. P. Zhang, L. Zhang, D. Tao, and X. Huang, "A multifeature tensor for remote-sensing target recognition," *IEEE Geosci. Remote Sens. Lett.*, vol. 8, no. 2, pp. 374–378, Feb. 2011.

[5] A. Samat, P. Gamba, S. Liu, P. Du, and J. Abuduwaili, "Jointly informative and manifold structure representative sampling based active learning for remote sensing image classification," *IEEE Trans. Geosci. Remote Sens.*, vol. 54, no. 11, pp. 6803–6817, Nov. 2016.

[6] P. S. Chavezm, Jr., S. C. Sides, and J. A. Anderson, "Comparison of three different methods to merge multiresolution and multispectral data: Landsat TM and SPOT panchromatic," *Photogramm. Eng. Remote Sens.*, vol. 57, no. 3, pp. 295–303, Mar. 1991.

[7] W. J. Carper, T. M. Lillesand, and R. W. Kiefer, "The use of intensity-hue-saturation transformations for merging SPOT panchromatic and multispectral image data ," *Photocrammetric Eng. Remote Sens.*, vol. 56, no. 4, pp. 459–467, Apr. 1990.

[8] C. A. Laben and B. V. Brower, "Process for enhancing the spatial resolution of multispectral imagery using pan-sharpening," U.S. Patent 6 011 875 A, Jan. 4, 2000.

[9] T.-M. Tu, P. S. Huang, C.-L. Hung, and C.-P. Chang, "A fast intensity-hue-saturation fusion technique with spectral adjustment for IKONOS imagery," *IEEE Geosci. Remote Sens. Lett.*, vol. 1, no. 4, pp. 309–312, Oct. 2004.

[10] B. Aiazzi, S. Baronti, and M. Selva, "Improving component substitution pansharpening through multivariate regression of MS+Pan data," *IEEE Trans. Geosci. Remote Sens.*, vol. 45, no. 10, pp. 3230–3239, Oct. 2007.

[11] Z. Wang, D. Ziou, C. Armenakis, D. Li, and Q. Li, "A comparative analysis of image fusion methods," *IEEE Trans. Geosci. Remote Sens.*, vol. 43, no. 6, pp. 1391–1402, Jun. 2005.

[12] S. Yang, M. Wang, and L. Jiao, "Fusion of multispectral and panchromatic images based on support value transform and adaptive principal component analysis," *Inf. Fusion*, vol. 13, no. 3, pp. 177–184, Jul. 2012.

[13] S. Rahmani, M. Strait, D. Merkurjev, M. Moeller, and T. Wittman, "An adaptive IHS pan-sharpening method," *IEEE Geosci. Remote Sens. Lett.*, vol. 7, no. 4, pp. 746–750, Oct. 2010.

[14] X. Otazu, M. González-Audícana, O. Fors, and J. Núñez, "Introduction of sensor spectral response into image fusion methods. Application to wavelet-based methods," *IEEE Trans. Geosci. Remote Sens.*, vol. 43, no. 10, pp. 2376–2385, Oct. 2005.

[15] V. P. Shah, N. H. Younan, and R. L. King, "An efficient pan-sharpening method via a combined adaptive PCA approach and contourlets," *IEEE Trans. Geosci. Remote Sens.*, vol. 46, no. 5, pp. 1323–1335, May 2008.

[16] B. Aiazzi, L. Alparone, S. Baronti, and A. Garzelli, "Context-driven fusion of high spatial and spectral resolution images based on oversampled multiresolution analysis," *IEEE Trans. Geosci. Remote Sens.*, vol. 40, no. 10, pp. 2300–2312, Oct. 2002.

[17] J. Nunez, X. Otazu, O. Fors, A. Prades, V. Pala, and R. Arbiol, "Multiresolution-based image fusion with additive wavelet decomposition," *IEEE Trans. Geosci. Remote Sens.*, vol. 37, no. 3, pp. 1204–1211, May 1999.

[18] H. Yin and S. Li, "Pansharpening with multiscale normalized nonlocal means filter: A two-step approach," *IEEE Trans. Geosci. Remote Sens.*, vol. 53, no. 10, pp. 5734–5745, Oct. 2015.

[19] S. Li and B. Yang, "A new pan-sharpening method using a compressed sensing technique," *IEEE Trans. Geosci. Remote Sens.*, vol. 49, no. 2, pp. 738–746, Feb. 2011.

[20] X. X. Zhu and R. Bamler, "A sparse image fusion algorithm with application to pan-sharpening," *IEEE Trans. Geosci. Remote Sens.*, vol. 51, no. 5, pp. 2827–2836, May 2013.

[21] S. Li, H. Yin, and L. Fang, "Remote sensing image fusion via sparse representations over learned dictionaries," *IEEE Trans. Geosci. Remote Sens.*, vol. 51, no. 9, pp. 4779–4789, Sep. 2013.

[22] C. Jiang, H. Zhang, H. Shen, and L. Zhang, "Two-step sparse coding for the pan-sharpening of remote sensing images," *IEEE J. Sel. Topics Appl. Earth Observ. Remote Sens.*, vol. 7, no. 5, pp. 1792–1805, May 2014.

[23] X. Meng, J. Li, H. Shen, L. Zhang, and H. Zhang, "Pansharpening with a guided filter based on three-layer decomposition," *Sensors*, vol. 16, no. 7, p. 1068, 2016.

[24] H. Li, F. Liu, S. Yang, K. Zhang, X. Su, and L. Jiao, "Refined pan-sharpening with NSCT and hierarchical sparse autoencoder," *IEEE J. Sel. Topics Appl. Earth Observ. Remote Sens.*, vol. 9, no. 12, pp. 5715–5725, Dec. 2016.

[25] K. Zhang, M. Wang, S. Yang, Y. Xing, and R. Qu, "Fusion of panchromatic and multispectral images via coupled sparse non-negative matrix factorization," *IEEE J. Sel. Topics Appl. Earth Observ. Remote Sens.*, vol. 9, no. 12, pp. 5740–5747, Dec. 2016.

[26] S. Yang, K. Zhang, and M. Wang, "Learning low-rank decomposition for pan-sharpening with spatial-spectral offsets," *IEEE Trans. Neural Netw. Learn. Syst.*, vol. 29, no. 8, pp. 3647–3657, Aug. 2018, doi: 10.1109/TNNLS.2017.2736011.

[27] H. Li, W. Li, G. Han, and F. Liu, "Coupled tensor decomposition for hyperspectral pansharpening," *IEEE Access*, vol. 6, pp. 34206–34213, Jun. 2018.

[28] H. Li, F. Wu, and X. Zhang, "Fusion of multispectral and panchromatic images via local geometrical similarity," *Tehnički Vjesnik*, vol. 25, no. 2, pp. 546–552, Apr. 2018, doi: 10.17559/TV-20171023105844.

[29] T. Delleji, A. Kallel, and A. B. Hamida, "Multispectral image adaptive pansharpening based on wavelet transformation and NMDB approaches," *Int. J. Remote Sens.*, vol. 35, no. 19, pp. 7069–7098, Sep. 2014.

[30] J. Choi, D. Han, and Y. Kim, "Context-adaptive pansharpening algorithm for high-resolution satellite imagery," *Can. J. Remote Sens.*, vol. 38, no. 1, pp. 109–124, Jan. 2012.

[31] A. Kallel, "MTF-Adjusted pansharpening approach based on coupled multiresolution decompositions," *IEEE Trans. Geosci. Remote Sens.*, vol. 53, no. 6, pp. 3124–3145, Jun. 2015.

[32] M.-Y. Liu, O. Tuzel, S. Ramalingam, and R. Chellappa, "Entropy rate superpixel segmentation," in *Proc. 24th IEEE Conf. Comput. Vis. Pattern Recognit. (CVPR)*, Colorado Springs, CO, USA, Jun. 2011, pp. 2097–2104.

[33] G. Vivone *et al.*, "A critical comparison among pansharpening algorithms," *IEEE Trans. Geosci. Remote Sens.*, vol. 53, no. 5, pp. 2565–2586, May 2015.

[34] A. Garzelli, F. Nencini, and L. Capobianco, "Optimal MMSE pan sharpening of very high resolution multispectral images," *IEEE Trans. Geosci. Remote Sens.*, vol. 46, no. 1, pp. 228–236, Jan. 2008.

[35] A. Garzelli, "Pansharpening of multispectral images based on nonlocal parameter optimization," *IEEE Trans. Geosci. Remote Sens.*, vol. 53, no. 4, pp. 2096–2107, Apr. 2015.

[36] S. G. Mallat, "A theory for multiresolution signal decomposition: The wavelet representation," *IEEE Trans. Pattern Anal. Mach. Intell.*, vol. 11, no. 7, pp. 674–693, Jul. 1989.
[37] Z. Wang and A. C. Bovik, "A universal image quality index," *IEEE Signal Process. Lett.*, vol. 9, no. 3, pp. 81–84, Mar. 2002.
[38] R. H. Yuhas, A. F. H. Goetz, and J. W. Boardman, "Discrimination among semi-arid landscape endmembers using the spectral angle mapper (SAM) algorithm," in *Proc. Summaries 3rd Annu. JPL Airborne Geosci. Workshop*, 1992, pp. 147–149.
[39] L. Alparone, S. Baronti, A. Garzelli, and F. Nencini, "A global quality measurement of pan-sharpened multispectral imagery," *IEEE Geosci. Remote Sens. Lett.*, vol. 1, no. 4, pp. 313–317, Oct. 2004.
[40] L. Wald, *Data Fusion. Definitions and Architectures—Fusion of Images of Different Spatial Resolutions*. Paris, France: Les Presses de l' Écoledes Mines, 2002.

HONG LI received the M.S. degree in computer application technology from Northwest University for Nationalities, Lanzhou, China, in 2006, and the Ph.D. degree in computer application technology from Xidian University, Xi'an, China, in 2016.

Her main current research interests include image processing and pattern recognition.

SHUYING LIU received the M.S. degree from Xi'an Shiyou University, China, in 2007.

Her research interests include image processing.

QUN DUAN is with the School of Computer Science, Xianyang Normal University, Xianyang, China.

Her research interests include image processing.

WEIBIN LI received the B.S. and M.S. degrees in mathematics from Northwest University, China, in 1998 and 2000, respectively, and the Ph.D. degree in circuits and systems from Xidian University, Xi'an, China, in 2004. In 2007, he received the title of Professor in computer science.

His research interests include satellite remote sensing image processing, satellite position and navigation, and space–time big data.